

LOW FREQUENCY MECHANICAL RESONANCE OF THE VOCAL TRACT IN VOCAL EXERCISES THAT APPLY TUBES

J. Horáček¹, V. Radolf¹, A.-M. Laukkanen²

¹Institute of Thermomechanics, The Academy of Sciences of the Czech Republic, Prague, Czech Republic

²Speech and Voice Research Laboratory, University of Tampere, Finland
jaromirh@it.cas.cz, Anne-Maria.Laukkanen@uta.fi, radolf@it.cas.cz

Jaromír Horáček, Institute of Thermomechanics AS CR, v. v. i., Dolejškova 1402/5, 182 00 Prague, Czech Republic, jaromirh@it.cas.cz, Tel. +420 26605 3125, **corresponding author**

Vojtěch Radolf, Institute of Thermomechanics AS CR, v. v. i., Dolejškova 1402/5, 182 00 Prague, Czech Republic, radolf@it.cas.cz,

Anne-Maria Laukkanen, Speech and Voice Research Laboratory, School of Education, Åkerlundink. 5, University of Tampere, 33100 Tampere, Finland, Anne-Maria.Laukkanen@uta.fi

Keywords: Biomechanics of voice; vocal tract acoustics; phonation into tubes; water resistance voice therapy; bubbling frequency; formant frequencies

Abstract:

Phonation into a tube that lowers the acoustic vocal tract resonance frequency and increases vocal tract impedance is used in voice therapy to establish effortless voice production. Additionally, keeping the distal end of the tube in the water results in the water bubbling and a consequent oscillation of oral pressure. This may feel like a massage of the vocal tract and larynx.

A low frequency mechanical resonance of the vocal tract, F_m , could enhance the effect of tube therapy in two ways: 1) by lowering the first acoustic resonance closer to the fundamental frequency of phonation, and 2) by introducing a coalescence of F_m with the water bubbling frequency.

A mathematical model of acoustic-structural interaction is introduced to clarify F_m in the context of phonation into a tube with the distal end in air and in water. The numerical results from the model are compared with the resonance frequencies measured in a male subject phonating on the vowel [u:] into a glass resonance tube with the distal end in air and at 2 cm and 10 cm under water. The effects of phonation through the tube are demonstrated by registering oral air pressure and electroglottography, and by synchronous high-speed filming of the water bubbling.

The first computed acoustic resonance frequency decreased from $F_l = 200$ Hz for the tube end in air down to about $F_l = 175$ Hz for the tube end in water, which roughly agrees with the first formant frequency of c. 179 Hz that was experimentally found for the human vocal tract. Considering the mechanical resonance F_m of the vocal tract to be c. 66 Hz, as previously estimated from measurements of a closed vocal tract, then according to the mathematical model for the vocal tract prolonged by a rigid glass tube, this frequency drops to 23 Hz. When the tube is submerged in water, F_m drops further to $F_m = 8$ Hz for the resonance tube and to about $F_m = 10$ Hz for a longer and wider silicon Lax Vox tube. The results thus show that the mechanical resonance can be near the measured water bubbling frequency $F_b = 11$ -11.5 Hz.

The results suggest that the mechanical resonance of the vocal tract tissues enhances the effects of the tube during voice therapy.

1. Introduction

Phonation into tubes of various dimensions is used for voice training and therapy purposes (see e.g. [1-3]). Phonation into a glass resonance tube (24-28 cm in length, 8-9 mm in inner diameter) with the outer end of the tube in air has been used for the voice training of normal voiced subjects to improve loudness and voice quality [1,3]. The beneficial effect of the exercise has been explained by assuming that the prolongation of the vocal tract (VT) lowers the first acoustic resonance of the vocal tract (first formant, F_1) near the fundamental frequency (F_0) in speech. This increases the positive reactance of the vocal tract at the F_0 range, which in turn has been found to assist vocal fold vibration mechanically [4]. Increased reactance decreases the phonation threshold and increases the amplitude of the harmonics without the use of excessive vocal fold collision. Thus, it improves the economy and efficiency of phonation (see e.g. [5,6]). The use of semi-occlusions, e.g. phonation into tubes or the production of voiced fricatives, nasals, and lip and tongue trills, increases the air pressure in the vocal tract. In such conditions, one feels the resonance vibrations in the vocal tract more clearly. It is assumed that during phonation into a tube, one becomes accustomed to how economic and efficient voice production feels and learns to use sensations of resonatory vibrations of the vocal tract tissues in order to monitor voice quality also when the tube is removed from the lips [6,7]. According to mathematical modelling results [8], F_1 is approximately in the range of ordinary speech, i.e. 200-300 Hz, for phonation into hard-walled tubes of 10 cm and 30 cm in length and with an inner diameter of 8 mm. The VT wall was considered to be yielding, having a mechanical resonance frequency (F_m) of its own. The parameters of such a VT model were set to the values suggested in [9], where the lowest acoustic resonance frequency of the closed VT was set to 200 Hz. However, it is plausible to suggest that this value can differ significantly when the VT is prolonged by a hard-walled tube with the distal end immersed in water.

It is known that the low mechanical resonance frequency (F_m) of the vocal tract is caused by the yielding walls of the VT cavities. Sondhi [10] postulated that this mechanical resonance is located below 20 Hz. The effect of the yielding walls is remarkable in speech produced in high ambient pressures, such as by deep-sea divers, and when the vocal tract is occluded or semi-occluded. The mechanical resonance causes shifts in the frequencies of the formants [8,9]. The authors of the papers [9,10] used the value $F_m = 15$ Hz in their computational modelling for the low mechanical resonance frequency of the vocal tract. This was deduced from the experimental data of formant frequencies and bandwidths measured by Fujimura & Lindqvist [11] for a closed vocal tract during plosive consonants. Ishizaka et al. [12] made direct measurements of VT wall impedance. According to their measurements, Liljencrants [13] formulated the dynamic properties of the mechanical resonances for the cheek and neck of a male subject, and estimated that the natural frequencies would range from 32 Hz for a relaxed cheek to 72 Hz for the neck.

Švec et al. [14] investigated the resonance properties of the laryngeal structures *in vivo*. Laryngeal vibrations were excited via a shaker placed on the neck of a male subject and observed by means of videostroboscopy and videokymography. The resonance frequency of the ventricular folds was found to be close to 70 Hz. The aryepiglottic folds and arytenoid cartilages were suspected to have resonances below 50 Hz, because when a sinusoidal excitation of 50 Hz was applied, large oscillations of the laryngeal collar were seen. The vocal folds oscillated as a unit with other laryngeal structures.

Large vibration amplitudes at frequencies of 50 Hz caused uncomfortable sensations in the subject, so measurements for frequencies lower than 50 Hz were not performed.

Therefore, it is known that there is a mechanical resonance (or resonances) below c. 70 Hz in the vocal tract. The role of this resonance becomes more prominent in phonation when the vocal tract is occluded or semi-occluded, as in the production of closed vowels, voiced consonants, or phonation into tubes, especially if the outer end of the tube is inserted into water, as in water resistance therapy [3].

Earlier studies by the authors [15,16] proved that the soft tissues of the human VT cavities had a considerable effect on the first formant frequency F_1 when the VT was prolonged by a tube. The measured F_1 for the VT model with hard walls corresponded to the computed value of 78 Hz. The experiments with a human subject instead resulted in a much higher value of F_1 , at about 200 Hz. The results confirm that a VT model with yielding walls must be considered for the mathematical modelling of human voice production.

Recently, many studies have also focused on water resistance voice therapy, where the subject phonates into a tube (either a glass resonance tube or a silicon Lax Vox tube), the outer end of which is submerged in water (see e.g. [17-19]). Such an exercise increases vocal tract impedance, and the impedance can be regulated by changing the depth the tube is immersed in the water. Bubbling frequency can be used to control the steadiness and rate of expiratory airflow. Water bubbling has been reported to feel like a massage, and it has been suggested that it could have the positive effects of massage (see e.g. [20,21]). In water resistance therapy, the mechanical low-frequency resonance of the soft tissue in the larynx could play an even more important role than for phonation on (semi-)occluded speech sounds or through a tube in air.

An experimental study [22] on gas bubble formation in water showed that the bubbling frequency F_b increases with flow rate from $F_b \cong 0$ at a nearly zero flow rate (“static bubble”) to a maximum value F_{bmax} depending on the inner diameter d of the tube orifice. For orifices from $d = 0.34$ -15.8 mm and flow rates from $Q = 0.01$ ml/s to $Q = 0.25$ l/s, the maximum bubbling frequency was found to range from about $F_{bmax} = 25$ Hz for the largest orifices to about $F_{bmax} = 75$ Hz for the smallest orifices. It was also found that water container widths from 3 to 10 square inches had no effect, and that the orifice submergences from about 2.54 cm to about 25.4 cm had a negligible effect on the bubbling process. The dimensions of the tubes used in water resistance therapy as well as the airflow rates typically used in speech are within the range of the parameters studied in [22].

Based on the above-mentioned earlier findings, we first hypothesize that the lowest mechanical resonance F_m of the vocal tract can raise F_1 during vocal exercising through a tube with its outer end in air. Therefore, F_m may affect the efficacy of the exercise. Second, we hypothesize that F_m may support the effect of water bubbling in water resistance voice therapy. Consequently, either a more efficient massage-like effect or even unpleasant sensations could be perceived on the vocal tract and vocal fold tissues when the bubbling frequency F_b is close to or coincides with the lowest mechanical resonance F_m of the vocal tract.

In order to test the hypotheses, we introduce here an improved mathematical model of the human vocal tract prolonged by a hard-walled tube. In the calculations, we will take into account the acoustic-structural interaction, which can help to clarify the physical background of the influence of the soft tissues of the vocal cavities on the formant frequencies.

2. Methods

2.1 Theoretical and mathematical background of the numerical modelling

Let us consider a coupled mechanical-acoustical system consisting of vocal tract cavity 1 and tube 2 with a cross-sectional area S_2 and a length L_2 (see Fig. 1). The glottis is closed by a yielding wall that has a mass m_w and vibrates with a displacement $w(t)$ on a spring of stiffness k_w and a damper b_w . The yielding wall with a cross-sectional area S_0 may consist of the soft tissue in the larynx, for example, the whole vocal folds body vibrating predominantly in a vertical direction inside the larynx or the larynx itself. Other walls of both the vocal tract and the tube are considered to be hard.

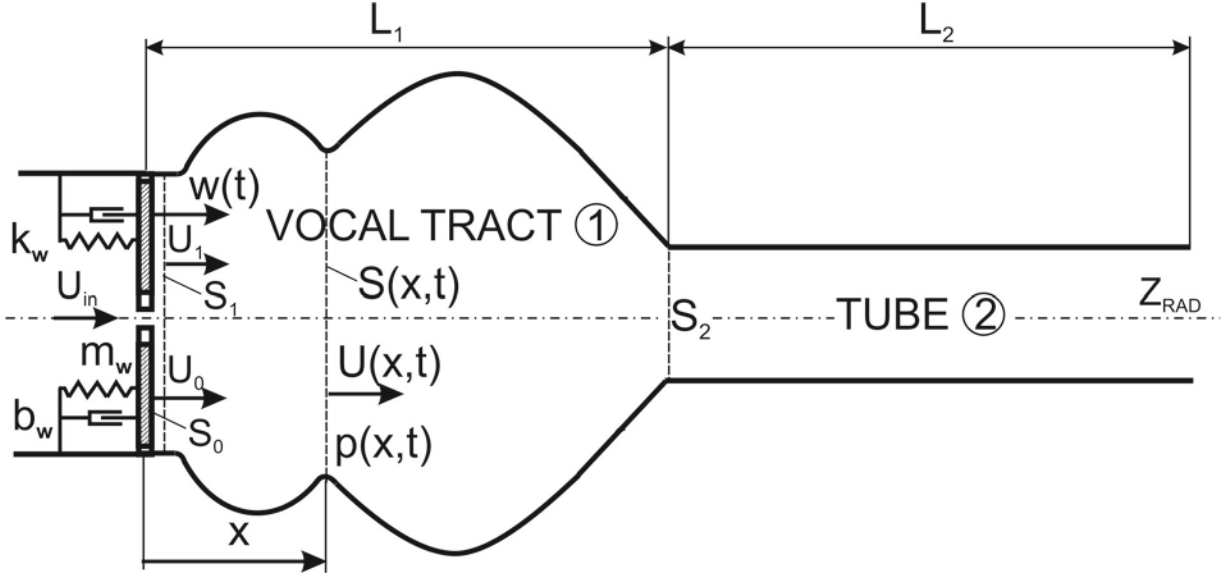


Fig. 1. Schema of the vocal tract model for vowel phonation through a tube connected to the lips. The inner end of the VT is closed by a yielding wall at the position of the vocal folds. The yielding wall is modelled by a damped dynamic mechanical system with one degree of freedom coupled with the VT model prolonged by the tube. The radiation losses are considered at the distal end of the tube.

The wave equation for air in the acoustic cavities of the vocal tract can be written as (see e.g. [23])

$$\frac{\partial^2 \varphi}{\partial x^2} + \frac{1}{S} \cdot \frac{\partial S}{\partial x} \cdot \frac{\partial \varphi}{\partial x} - \frac{1}{c_0^2} \cdot \left(\frac{\partial^2 \varphi}{\partial t^2} + c_0 \cdot r_N \cdot \frac{\partial \varphi}{\partial t} \right) = 0, \quad (1)$$

where φ is the flow velocity potential related to the acoustic pressure p and the acoustic volume velocity U as

$$p = -\rho_0 \frac{\partial \varphi}{\partial t} - c_0 \rho_0 r_N \varphi, \quad U = S \frac{\partial \varphi}{\partial x}, \quad (2)$$

where x is the longitudinal coordinate along the VT, t is time, c_0 is the speed of sound, ρ_0 is the air density inside the VT, and $S(x,t)$ is the cross-sectional area of the acoustic cavity at the distance x from the vocal folds.

Specific acoustic resistance r_N due to fluid dynamic viscosity μ is defined as (see [24])

$$r_N = \frac{1}{c_0 R(x)} \sqrt{\frac{2 \omega \mu}{\rho_0}}, \quad (3)$$

where $R(x)$ is the radius of an acoustic element that is a part of the acoustic wave guide (VT + tube) of the length L_1+L_2 and ω is the angular frequency (see Fig. 1).

The model presented in Fig. 1 takes into consideration the sound radiation from the tube end to the surrounding space respecting the second source of dissipation losses during phonation. These radiation losses can be modelled by a circular plate vibrating like a piston in an infinite wall, for which the following frequency-dependent acoustic impedance can be derived (see e.g. [24]):

$$Z_{RAD} \equiv \frac{p_{out}}{U_{out}} = \frac{c_{out} \rho_{out}}{\pi R_{out}^2} \left(1 - \frac{J_1(2k R_{out})}{k R_{out}} + j \frac{H_1(2k R_{out})}{1 + k R_{out}} \right), \quad (4)$$

where c_{out} is sound velocity, and ρ_{out} is the fluid density in the surrounding space, R_{out} is the inner radius at the distal end of the tube, $k = \omega/c_{out}$ is the wave number, J_1 and H_1 are the Bessel and Struve functions of order 1 and $j = \sqrt{-1}$ is the imaginary unite.

The relation between the amplitudes of the acoustic pressure p and the volume velocity U at the input and output of the complete VT with the tube can be described by a global transfer matrix as (see [16,23])

$$\begin{bmatrix} p_{out} \\ U_{out} \end{bmatrix} = \begin{bmatrix} A & B \\ C & D \end{bmatrix} \cdot \begin{bmatrix} p_1 \\ U_1 \end{bmatrix}, \quad (5)$$

where A , B , C , and D are components of the transfer matrix of the complete acoustic system (VT + tube), which was divided into 31 acoustic elements (1 short cylindrical element created by a very thin air layer on the surface S_1 of the yielding wall, 29 conical acoustic elements for the VT, and 1 cylindrical element for the tube with the inner radius R_{out}).

From eqs. (4) and (5) and using the relation $AD - BC = 1$ for the global transfer matrix (see e.g. [23]), we obtain the relations:

$$\text{a) } p_{out} = \frac{Z_{RAD}}{A - C \cdot Z_{RAD}} \cdot U_1, \quad \text{b) } p_1 = \frac{D \cdot Z_{RAD} - B}{A - C \cdot Z_{RAD}} \cdot U_1. \quad (6)$$

The volume airflow velocities and the air pressure in the first thin acoustic element must satisfy the conditions:

$$\text{a) } U_{in} + U_0 - U_1 = 0 \quad \text{b) } p_{in} = p_1. \quad (7)$$

The vibration of the yielding wall is given by the equation of the motion of the dynamic system with one degree of freedom:

$$m_w \ddot{w}(t) + b_w \dot{w}(t) + k_w w(t) + p(x=0, t) S_0 = 0, \quad (8)$$

where \dot{w} and \ddot{w} denote the first and the second time derivative of w , respectively, and the pressure in the first acoustic element in the vocal tract is loading the surface S_0 of the mass m_w by the force $p(x=0, t) S_0$.

The relation between the velocity of the mechanical system and the acoustic volume velocity U can be described as

$$\dot{w} = U(x=0, t) / S_0. \quad (9)$$

Considering the harmonic signal of angular frequency ω , the solution for the displacement w is supposed to be

$$w(t) = w_0 \cdot e^{j\omega t} \quad (10)$$

and we can write

$$v = j\omega w_0 e^{j\omega t}, \quad \dot{w} = -\omega^2 w_0 e^{j\omega t} \quad \text{and} \quad j\omega w_0 = U_0 / S_0 \Rightarrow U_0 = S_0 j\omega w_0, \quad p(x=0, t) = p_1 e^{j\omega t} \quad (11)$$

Substitution of eqs. (9) – (11) into eq. (8) yields:

$$(j\omega m_w + b_w + k_w / j\omega) U_0 / S_0 + p_1 S_0 = 0. \quad (12)$$

Substituting p_1 from eq. (6b) and U_0 from eq. (7a) into eq. (12) gives

$$\left(j\omega m_w + b_w + \frac{k_w}{j\omega} \right) \frac{U_1 - U_{in}}{S_0^2} + \frac{D \cdot Z_{RAD} - B}{A - C \cdot Z_{RAD}} \cdot U_1 = 0, \quad (13)$$

from where the volume airflow velocity U_1 can be expressed as

$$U_1 = \left(j\omega m_w + b_w + \frac{k_w}{j\omega} \right) \frac{U_{in}}{S_0^2} \left[\frac{D \cdot Z_{RAD} - B}{A - C \cdot Z_{RAD}} + \left(j\omega m_w + b_w + \frac{k_w}{j\omega} \right) \frac{1}{S_0^2} \right]^{-1} \quad (14)$$

and substituting eq. (14) into eq. (6a), the transfer function between the output pressure $p(x=L_1+L_2)$ and the inflow volume velocity U_{in} can be derived as

$$p_{out} / U_{in} = \frac{Z_{RAD}}{S_0^2} \left(j\omega m_w + b_w + \frac{k_w}{j\omega} \right) \left[(D Z_{RAD} - B) + (A - C Z_{RAD}) \left(j\omega m_w + b_w + \frac{k_w}{j\omega} \right) \frac{1}{S_0^2} \right]^{-1}. \quad (15)$$

From the condition of zero denominator, we get the following frequency equation for computing the eigenfrequencies of the coupled acoustic-mechanical system:

$$\omega^2 + j\omega \left(\frac{B - D \cdot Z_{RAD}}{A - C \cdot Z_{RAD}} \cdot \frac{S_0^2}{m_w} - 2\zeta_w \omega_w \right) - \omega_w^2 = 0, \quad (16)$$

where $\omega_w^2 = k_w / m_w$ is the squared angular frequency of mechanical resonance, $\zeta_w = b_w / (2m_w \omega_w)$ is the damping ratio of the yielding wall, and Z_{RAD} is the radiation impedance at the distal end of the tube.

The numerical solutions were performed for phonation with a resonance tube or Lax Vox tube into air and into water, and the VT geometrical configuration corresponded to the Czech vowel /u:/ (see Fig 2). The circular cross-sectional areas of the radius $R(x)$, perpendicular to the midline along the vocal tract from the vocal folds situated at $x = 0$ up to the lips located at $x = L_l$, were obtained from the magnetic resonance images (MRI) recorded during the phonation of the male subject (see [25]).

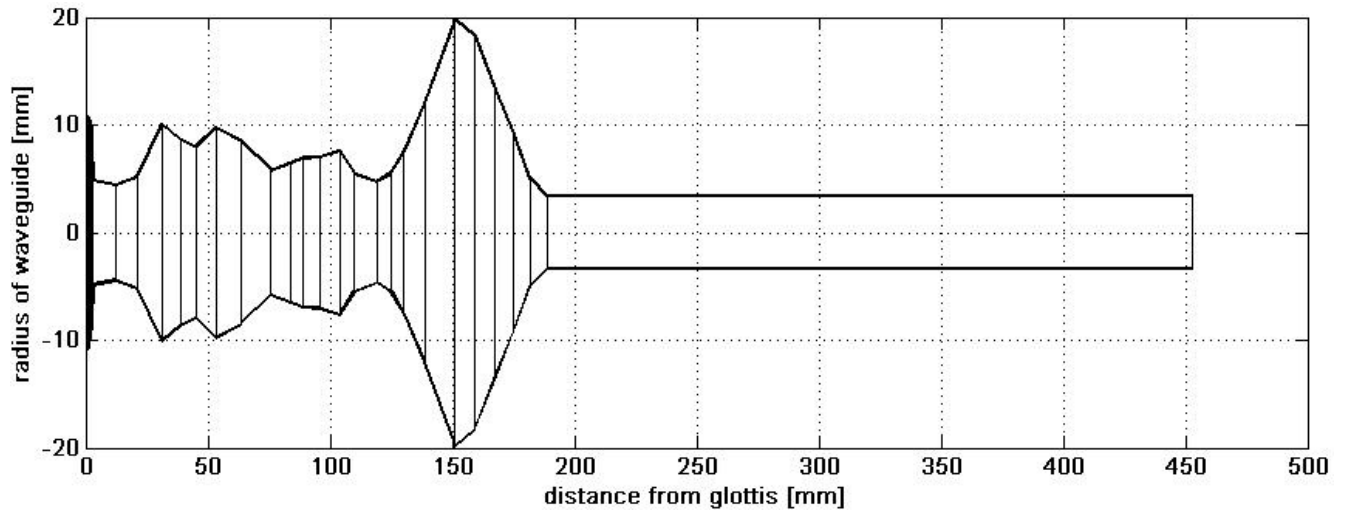


Fig. 2. Geometry of the vocal tract model for vowel /u:/ designed from conical acoustic elements when the vocal tract is prolonged by a tube.

The following input parameters were considered for air: the density $\rho_0 = 1.2 \text{ kgm}^{-3}$, speed of sound $c_0 = 353 \text{ m/s}$, dynamic viscosity $\mu = 1.8 \cdot 10^{-5} \text{ Pa s}$; and for water: $\rho_{out} = 998 \text{ kgm}^{-3}$, $c_{out} = 1500 \text{ m/s}$.

The geometrical parameters considered for the resonance tube were $L_2 = 26.4 \text{ cm}$ and $S_2 = 0.36 \text{ cm}^2$, which corresponds to an inner diameter of 6.8 mm. For the Lax Vox tube, the parameters were $L_2 = 35 \text{ cm}$ and $S_2 = 0.785 \text{ cm}^2$, which corresponds to an inner diameter of 10 mm. The following areas were considered: $S_0 = 3.78 \text{ cm}^2$ for the mechanical system and $S_1 = 3.80 \text{ cm}^2$ for the first acoustic element at the glottis (see Figs. 1 and 2).

The following parameters for the mechanical system were recalculated from the data published by Liljencrants [13 – Table 4.1]: the eigenfrequency $\omega_w = 2\pi \cdot 66 \text{ rad/s}$, the damping ratio of the yielding wall $\zeta_w = 0.99$, and the mass $m_w = 1400 S_0^2 = 0.2 \text{ gram}$, which corresponds to the mass of the yielding wall considered in the authors' previous paper [16].

2.2 Experiment: Phonation through a tube with the outer end in air or submerged in water

One male volunteered as a subject. He phonated on [u:] at a comfortable pitch and loudness into a glass resonance tube (26.4 cm in length, 6.8 mm in inner diameter) with the outer end of the tube in air and submerged at 2 cm and 10 cm under water.

The sound pressure level (SPL) inside the oral cavity was measured using a special microphone probe designed for the measurement of acoustic pressure in small cavities (B&K 4182), and the mean oral pressure (P_{oral}) was measured with a digital manometer (Greisinger Electronic GDH07AN) connected to the oral cavity by a small compliant tube (inner diameter 1.5 mm, length 8 cm), the end of which was positioned at the corner of the subject's mouth similarly as the microphone probe. The nose was closed with a clip to prevent any leakage of air. The electroglottographic (EGG) signal, which shows the varying contact of the vocal folds during phonation, was registered using a dual channel device (Glottal Enterprises). The acoustic signal outside the vocal tract was recorded using a sound level meter (B&K 2239A). The recording was made with a 16.4 kHz sampling frequency using the PC-controlled measurement system B&K PULSE 10. The audio recording was synchronized with

a high-speed camera that registered the water bubbling at a rate of 1,000 frames per second. The frequency range of the digital manometer started at 0 Hz, but attenuated gradually towards frequencies above c. 80 Hz. The microphone probe was set to function in the range from 20 Hz to its upper limit of 20 kHz. This means that the quite low frequency of bubbling F_b could not be detected by the microphone probe properly. However, fundamental frequencies of the vibrating vocal folds F_0 , which were above 100 Hz, were correctly recorded by this probe.

The subglottal pressure (P_{sub}) during sustained phonation into the tube was estimated by measuring the pressure in the oral cavity when the cavity was manually shuttered at the distal end of the tube. P_{sub} was read from the time signal just when the tube end was closed, the glottis was opened, and the vocal folds had stopped vibrating – i.e. when the air pressure in the oral cavity was equal to the pressure in the lungs. This shuttering was repeated several times during each trial, which was 10 s long in total.

The acoustic analysis of the measured pressure signals was done by averaging the fast Fourier transform (FFT) frequency spectra computed by a Hanning window of 1 s with a 75% overlap. The resulting averaged (filtered) spectra were obtained by using frequency bands (windows) that were equal to the fundamental phonation frequency F_0 and shifting them by a frequency step Δf . The maxima of these “filtered spectra” determine the resonance (formant) frequencies of the vocal tract cavities (see the Appendix for more details).

3. Results

3.1 Numerical simulations

The complex eigenfrequencies of the coupled acoustic-structural system (see Figs. 1 and 2) were computed from the frequency equation (16). The magnitudes (absolute values) of the first two eigenfrequencies’ dependence on the length $L_2 = 0$ -50 mm and the inner diameter $d = 2$ -16 mm of the tube with its outer end in air or submerged in water are shown in Figs. 3 and 4, respectively.

The vocal tract alone (for $L_2 = 0$), having a volume of 57 cm³, contains c. 0.065 grams of air, which is an added mass to that of the yielding wall and reduces the first frequency F_m of the predominantly mechanical resonance to the frequency range 38-46 Hz depending on the diameter d of the mouth opening (see Fig. 3a). When the tube of length $L_2 = 50$ cm is connected, the total mass of the air increases to 0.07-0.19 grams, and due to the added fluid mass, the frequency F_m is further reduced down to the frequency range 5-32 Hz depending on the tube diameter. We can note that by increasing the tube length, the radiation effect, given in eq. (16) by the quantity Z_{RAD} at the distal end of the tube, is a constant.

The second frequency F_1 , corresponding to a predominantly acoustic resonance, which is important for the most efficient voice production, changes with the length and diameter of the tube in a similar manner as the frequency F_m . For the vocal tract alone, i.e. for $L_2 = 0$, the frequency F_1 corresponds to the first so-called formant frequency for the vowel [u:], which is in the frequency range 290-550 Hz depending on the diameter d of the mouth opening (see Fig. 3b). This frequency decreases with the tube length to 175-185 Hz for $L_2 = 50$ cm.

The computed natural frequencies dependent on the length and the inner diameter of the tube with its outer end submerged in water are shown in Fig. 4. All frequencies are substantially reduced compared to the situation when the distal end of the tube is in air. This is due to a substantial difference in the radiation condition (4) at the tube end.

The frequency F_m of the predominantly mechanical resonance for the vocal tract alone, i.e. for $L_2 = 0$, is further reduced to the frequency range 4.5-12.5 Hz depending on the diameter d of the mouth opening (see Fig. 4a). When a tube of length $L_2 = 50$ cm is connected to the VT, the frequency F_m is further reduced down to the frequency range 3.4-11.5 Hz depending on the tube diameter.

All frequencies decrease as the tube length increases. The changes of the natural frequencies with the diameter are more complicated. The predominately mechanical resonance frequency F_m increases with the tube diameter for the tube end both in air and in water. The predominately acoustic resonance F_1 varies with tube diameter differently for the tube end in air and for the tube end in water. This resonance increases with the tube diameter for the tube end in air, while a completely opposite trend is visible for the tube end in water (see Figs. 3b and 4b).

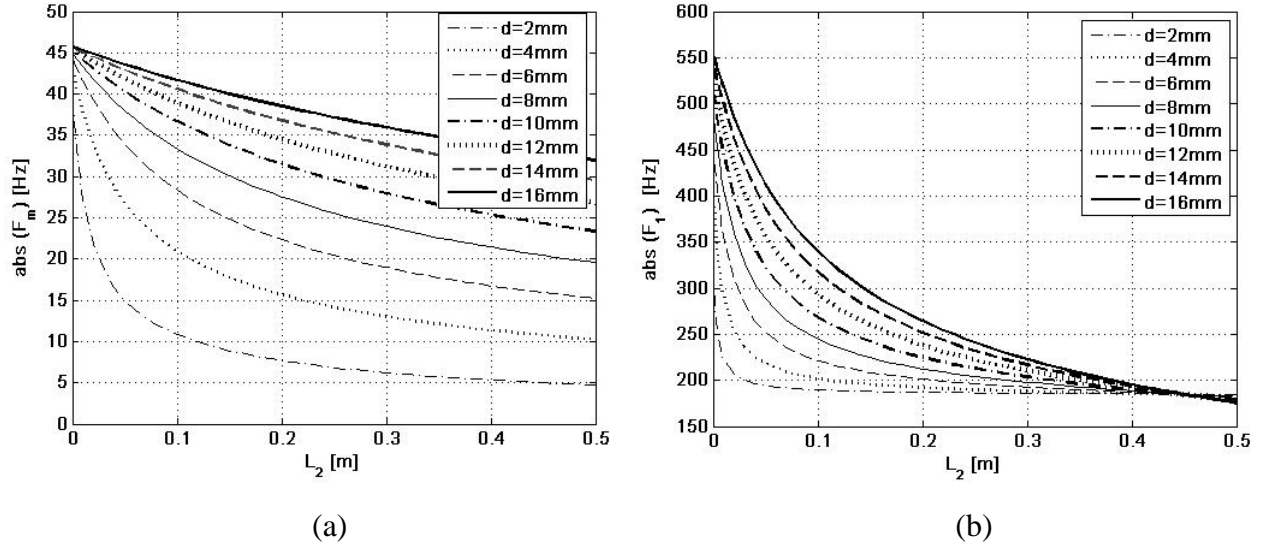


Fig. 3. Dependence of the first two computed magnitudes (absolute values) of the natural frequencies (F_m and F_1) of the model on the length L_2 and inner diameter d of the tube with the distal end in air.

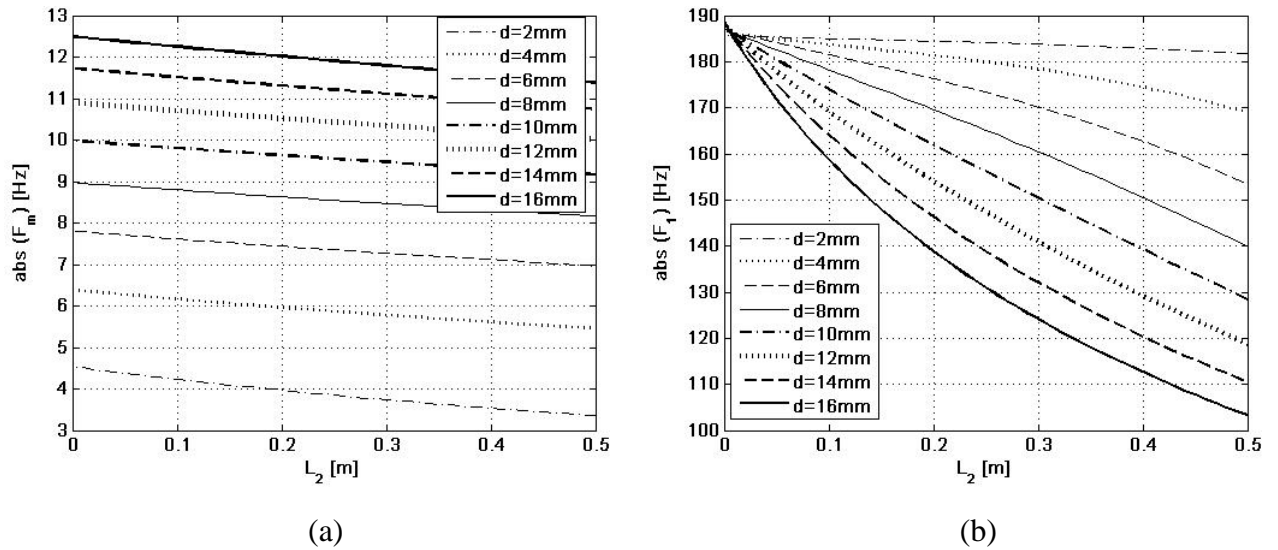


Fig. 4. Dependence of the first two computed magnitudes (absolute values) of the natural frequencies (F_m and F_1) of the model on the length L_2 and inner diameter d of the tube with the distal end in water.

Table 1 summarizes the first four computed complex eigenfrequencies for phonation into the resonance tube and into the Lax Vox tube in air and in water. We note that an important parameter that characterizes the damping properties of the acoustic and dynamic mechanical systems is the half-power (3 dB) frequency bandwidth of the resonance, which is equal to the double of the imaginary part of the complex eigenfrequency presented in Table 1.

Table 1. Computed complex eigenfrequencies for phonations in the resonance tube and the Lax Vox tube into air and into water (3dB frequency bandwidth = $2 f_{imag}$, where $F = f_{real} + j f_{imag}$).

| Resonance tube | F_m [Hz] | F_1 [Hz] | F_2 [Hz] | F_3 [Hz] |
|----------------------|----------------|------------------|------------------|------------------|
| Phonation into air | $20.6 + j 8.3$ | $195.0 + j 34.3$ | $647.0 + j 9.6$ | $789.0 + j 14.5$ |
| Phonation into water | $7.8 + j 0.9$ | $164.9 + j 37.5$ | $367.8 + j 8.4$ | $773.4 + j 15.4$ |
| Lax Vox tube: | | | | |
| Phonation into water | $9.3 + j 1.3$ | $141.2 + j 32.6$ | $313.7 + j 10.4$ | $714.6 + j 11.0$ |

Figure 5 presents the computed transfer functions (15) between the output pressure p_{out} at the distal end of the tube and the inflow volume velocity U_{in} exciting harmonically the VT model prolonged by the resonance tube and by the Lax Vox tube for phonation into air and into water. The transfer functions are very similar for the first two resonances (below 300 Hz) in phonation into the resonance tube and into the Lax Vox tube, and for both phonation into air and into water. The acoustic pressure response level is much higher for the tubes with the distal ends in water than in air, especially in the frequency range up to about 500 Hz. This corresponds to the increase of the radiation impedance (4) for the distal end of the tube in water, for which the absolute value of Z_{RAD} is about 800 times higher than for the distal end of the tube in air. The responses for the third and higher resonances are different for the two tubes, mainly because of the great difference in the length of the tubes. Structural damping significantly lowers the peaks of the first and second resonance frequencies, especially for the resonance tube in air. The first four resonance frequencies evaluated from the graphs in Fig. 5 are summarized in Table 2.

The resonance frequencies in Table 2 and the real part of the eigenfrequencies in Table 1 computed for phonation in the resonance tube and the Lax Vox tube into air and into water are in good agreement for the mechanical resonance frequency F_m and for the formant frequencies F_2 and F_3 . The differences are less than 5.7 % for the formant frequencies F_i ($i = 1, 2, 3$) and the greatest difference (10%) is for the mechanical resonance frequency F_m due to the considered strong structural damping.

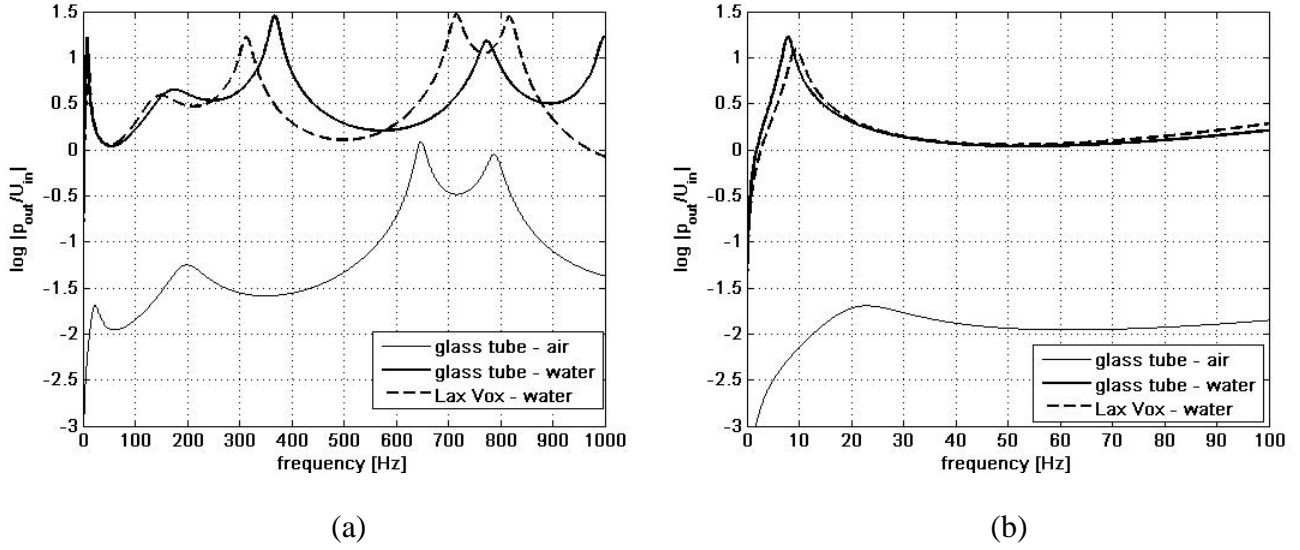


Fig. 5. Computed absolute values of the transfer functions p_{out}/U_{in} of the VT model for the vowel /u:/ prolonged by the resonance tube in air and in water and by the Lax Vox tube in water (a), with the detail in the frequency range of the first resonance (b).

Table 2. Computed resonance frequencies for phonations in the resonance tube and in the Lax Vox tube into air and into water.

| Resonance tube | F_m [Hz] | F_1 [Hz] | F_2 [Hz] | F_3 [Hz] |
|----------------------|------------|------------|------------|------------|
| Phonation into air | 22.9 | 199.9 | 648 | 788 |
| Phonation into water | 7.8 | 174.5 | 368 | 774 |
| Lax Vox tube: | | | | |
| Phonation into water | 9.4 | 149.0 | 313 | 716 |

3.2 Experimental investigation of phonation into a resonance tube with the outer end submerged in water

Examples of simultaneously recorded time signals for the vertical larynx position (VLP), the *EGG* signal, the oral air pressure (P_{oral}), and the images of the bubble formation are presented in Figs. 6 and 7 for the male subject during a comfortable phonation into the tube with the discharge orifice submerged 10 cm and 2cm deep in water, respectively. The time instants marked by small circles correspond to the images taken by the high-speed camera.

Figure 6 shows the VLP, *EGG*, and P_{oral} signals in the time domain for phonation into the tube submerged 10 cm in water ($P_{sub} = 1.8$ kPa and mean $P_{oral} = 1.02$ kPa). In all three signals, it is clearly possible to identify the low bubbling frequency $F_b = 11$ Hz and the fundamental frequency of phonation $F_0 = 98$ Hz. Oscillations caused by bubbling influence the oral air pressure, vertical larynx position, and also the contact area of the vocal folds, which can be seen in the *EGG* signal. The water bubbling affects the vertical position of the larynx, which is derived from an amplitude difference between the two pairs of electrodes used in the electroglottograph device. The peak-to-peak value of the oral pressure ($P_{oral\ ptp}$) is about 400 Pa, and the oral pressure P_{oral} varies simultaneously with the intensive vibrations of the larynx in a vertical direction.

The images numbered 533, 605, 696, and 788 in Fig. 6 correspond to the maxima of the oral pressure P_{oral} (marked by major circles). The images numbered 557, 638, 730, and 821 correspond to the minima of the oral pressure (marked by empty squares) and to the time instants of higher VLP values when the bubble separation from the tube orifice approximately begins, i.e. when the oral pressure is minimal, and the larynx is in the highest position. When the oral pressure increases, the larynx moves down, and conversely when the oral pressure decreases, the larynx moves up. The images numbered 577, 662, 750, and 845 correspond to the time instants just after the bubble separation from the tube end and a new air bubble starts to be created at the discharge orifice.

Similarly, Fig. 7 shows the results for the tube submerged 2 cm deep in water ($P_{oral} = 250$ Pa, $F_b = 11$ Hz, $F_0 = 98$ Hz). The images numbered 1343, 1445, 1526, and 1619 registered by the high-speed camera correspond to the maxima of the oral pressure, and the images numbered 1376, 1479, 1581, and 1653 correspond to the minima of the oral pressure. The changes in the VLP signal are not so regular as for the tube end immersion depth of 10 cm due to a more intensive boiling-like effect, when the waves on the water surface randomly change the hydrostatic pressure. The time instants of the bubble separation from the tube end are difficult to identify in this case because the bubbles reach the water level before separating from the tube end (see e.g. the images numbered 1479, 1581, and 1653). The separation period is not constant; the process is more irregular compared to the previous case because of the interaction of the air bubbles with the gravity waves on the water surface.

The frequency spectra of oral air pressure measured for the male subject during phonation into the resonance tube with the outer end submerged 10 cm and 2 cm deep in water are displayed in the frequency range 0-200 Hz in Fig. 8, captured both by the digital manometer and by the microphone probe. The oral pressure was measured correctly by the microphone probe B&K 4182 in the higher frequency range, and the mean oral pressure was measured correctly by the digital manometer GDH07AN in the lowest frequency region beginning from 0 Hz. The bubbling effect is attenuated in the pressure signal measured by the microphone probe, and the frequencies higher than about 100 Hz are attenuated in the pressure signal measured by the digital manometer. The frequency of bubbling $F_b = 11$ Hz as well as the fundamental frequency of vibrating vocal folds $F_0 = 98$ Hz are the same for the tube end submerged 10 cm and 2 cm under the water's surface. The maximum intensity, about 126 dB, is the same at the bubbling frequency F_b and at the fundamental phonation frequency F_0 in the case of the tube end submerged 10 cm in water. For the water depth 2 cm, the maximum intensity of about 128 dB is located at the fundamental frequency of vibrating vocal folds $F_0 = 98$ Hz.

Figure 9 shows the frequency spectra of oral air pressure measured by the microphone probe in the frequency range 0-1 kHz, where it is possible to identify the first two formant frequencies $F_1 \cong 179$ Hz and $F_2 = 330$ -340 Hz.

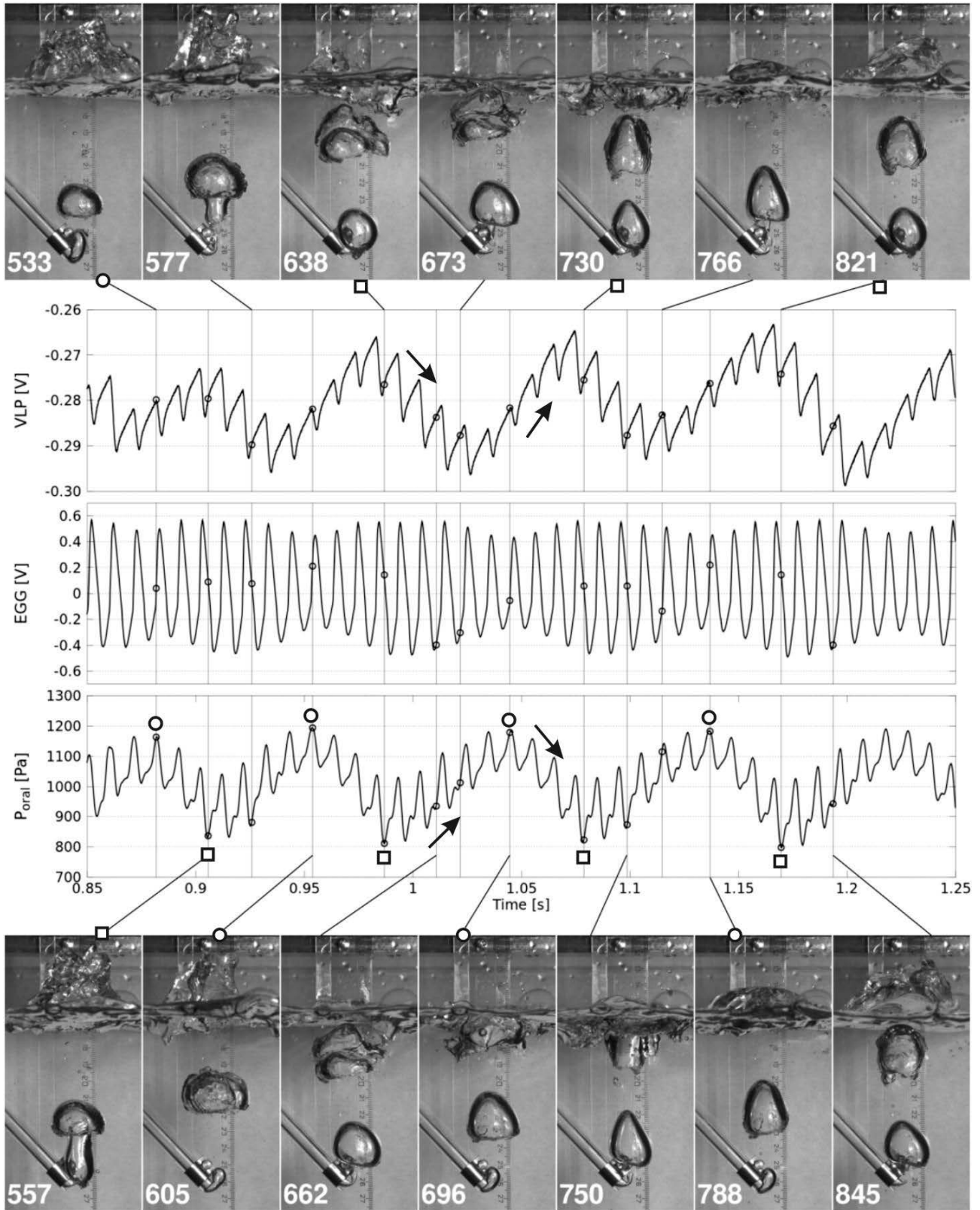


Fig. 6. Vertical larynx position (VLP), electroglottographic (EGG), and oral pressure (P_{oral}) signals, and images of the bubbling process taken by a high-speed camera at the time instants marked by small circles during a comfortable phonation into the resonance tube submerged 10 cm deep in water.

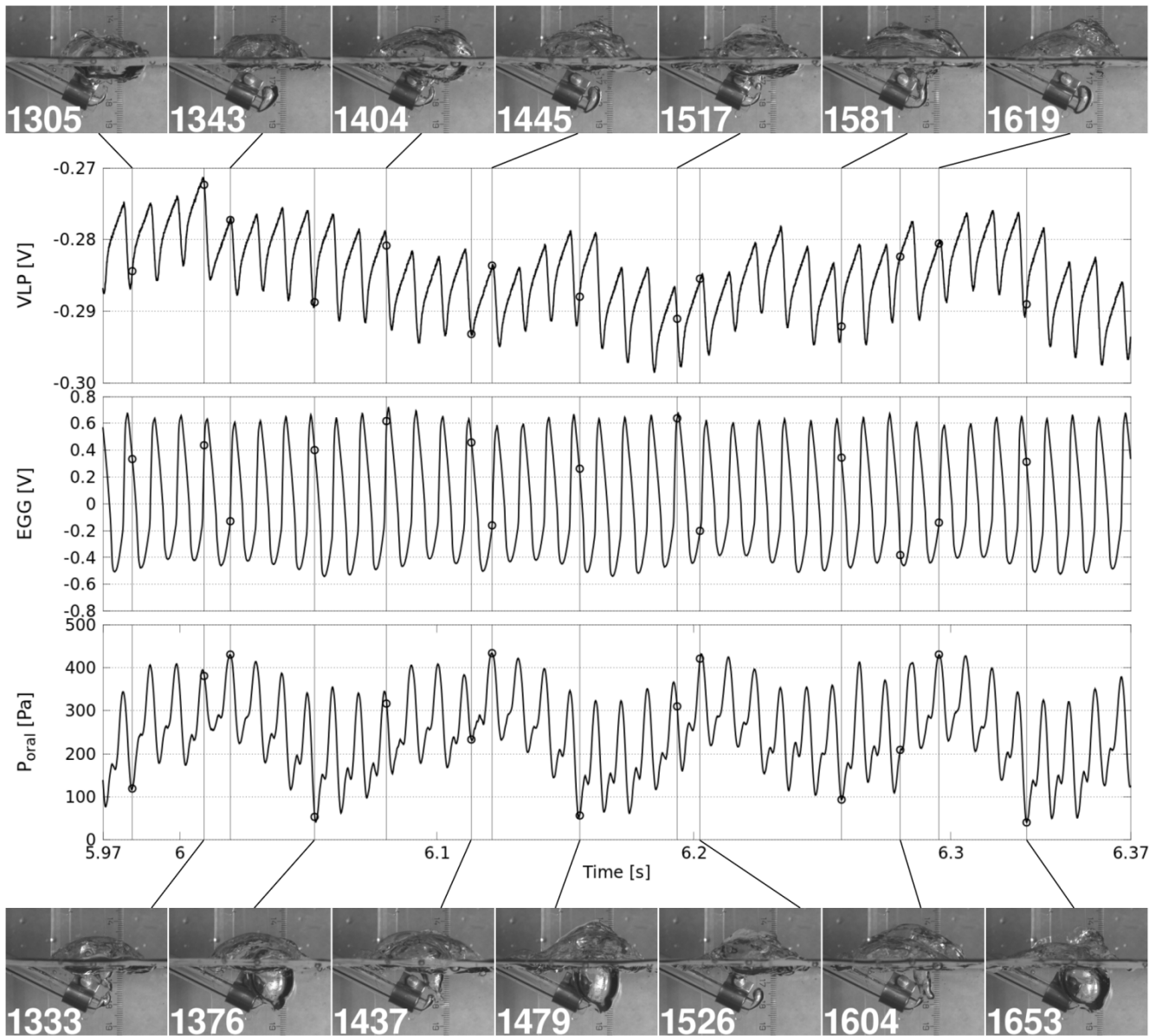
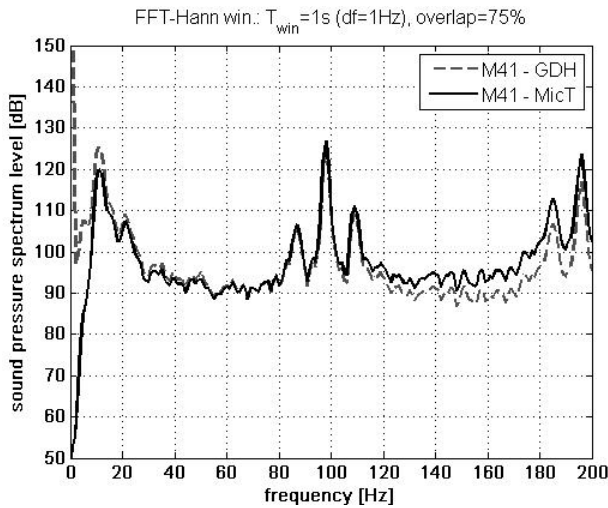
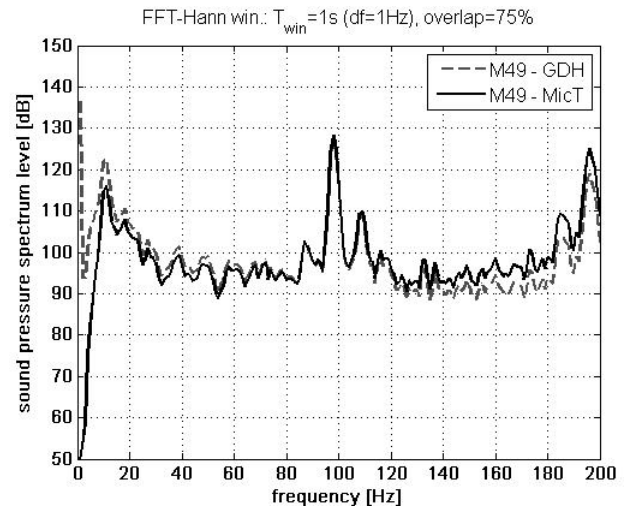


Fig. 7. Vertical larynx position (VLP), electroglottographic (EGG), and oral pressure (P_{oral}) signals, and images of the bubbling process taken by a high-speed camera at the time instants marked by small circles during a comfortable phonation into the resonance tube submerged 2 cm deep in water.

The results of the measurements are summarized in Table 3.

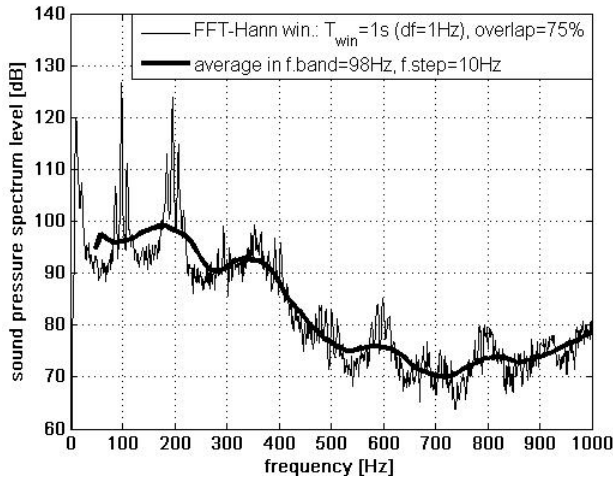


(a)

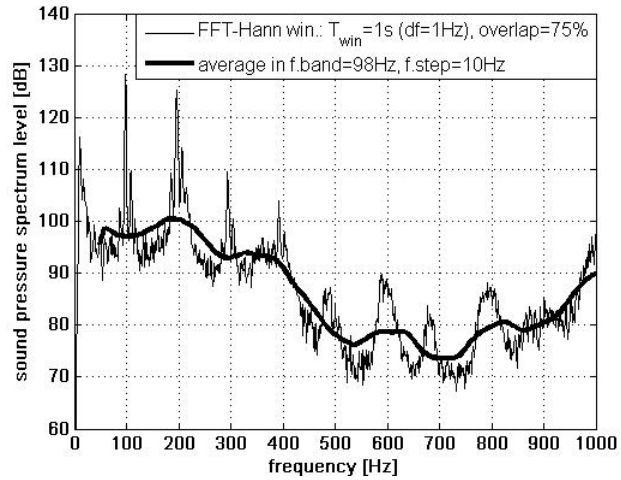


(b)

Fig. 8. Frequency spectra of the oral air pressure signal registered by microphone probe, not attenuated in the higher frequency range (full line), and by digital manometer, not attenuated in the lowest frequency region (dashed line) during a comfortable phonation into the resonance tube submerged 10 cm (a) and 2 cm (b) deep in water.



(a)



(b)

Fig. 9. Frequency spectra of oral air pressure signal registered by microphone probe during comfortable phonation into the resonance tube submerged 10 cm (a) and 2 cm (b) deep in water.

Table 3. Measured subglottal pressure (P_{sub}), mean oral pressure (P_{oral}), peak-to-peak oral pressure ($P_{oral,ptp}$), frequencies for bubbling (F_b), fundamental (F_0) and the first two formants (F_1 , F_2), and measured 3 dB frequency bandwidth B_1 for phonations into the resonance tube in air and in water with the distal end of the tube 2 and 10 cm deep (x: undefinable value).

| Resonance tube | P_{sub} [Pa] | P_{oral} [Pa] | $P_{oral,ptp}$ [Pa] | F_b [Hz] | F_0 [Hz] | F_1 [Hz] | B_1 [Hz] | F_2 [Hz] |
|--|-------------------|--------------------|------------------------|---------------|---------------|---------------|---------------|---------------|
| phonation into air | 600 | 25 | 210 | / | 100 | 190 | 138 | x |
| phonation into water (deepness 2 cm) | 910 | 249 | 397 | 11.0 | 98 | 179 | 117 | 330-340 |
| phonation into water (deepness 10 cm) | 1 800 | 1 019 | 391 | 11.5 | 98 | 179 | 135 | 330-340 |

4. Discussion

4.1 Experimental results

Phonation into the resonance tube submerged under the water's surface substantially influences the oral-air pressure and vibration pattern of the vocal folds by the formation of bubbles and their separation from the distal end of the tube. These changes show a periodic character with a frequency of 11 Hz for tube submersion depths of both 10 cm and 2 cm under the water's surface. The maximum intensity at the bubbling frequency in the spectra of the oral pressure signal is comparable to the amplitude of the first harmonic, corresponding to the vibration of the vocal folds at the fundamental frequency (see Fig. 9).

We can note that very similar results as those presented in Figs. 6 and 7 were obtained in a previous study by the authors [26] for a female subject phonating comfortably into an identical resonance tube as considered here with the distal end submerged 10 cm and 2 cm in water. The measured frequencies of bubbling, $F_b = 13$ Hz and $F_b = 16$ Hz, dominated in the spectra of the oral pressure signals, being about 15 dB stronger than the amplitude at the fundamental frequency $F_0 = 165$ Hz. The low bubbling frequencies were also visible as clear periodic changes in the VLP signals, which were obtained in the same way as presented here, i.e. with a dual-channel EGG.

The results in Table 3 for the male subject studied here show that the peak-to-peak value of the oral pressure variation ($P_{oral,ptp}$) does not depend on the depth of the submersion of the tube in water, which is obvious from the fact that the differences for the peak-to-peak values of the oral pressure between submersion depths 2 cm and 10 cm in water were small, 397 Pa for 2 cm and 391 Pa for 10 cm. This finding is in line with the results in [27]. We can also remark that the male subject phonated with an identical fundamental frequency $F_0 = 98$ Hz and had nearly identical first two resonance (formant) frequencies in both of the cases studied here. Thus, the only substantial differences between phonation into the tube with the distal end either 10 cm or 2 cm in the water were observed in the subglottal pressure and the mean oral pressure, as could be expected. Because neither P_{sub} nor P_{oral} are included as input parameters in the computational modelling of the acoustic characteristics of the system studied here, the numerical results presented are valid for both water depths considered in the experiments.

The results of the acoustic resonances obtained here suggest that phonation through a tube in water would decrease the frequency difference $F_1 - F_0$ down from 90 Hz to 81 Hz (see Table 3). Thus, water resistance voice therapy enhances acoustic interaction. The results are in contrast with those obtained

in [28], where it is reported that the difference $F_1 - F_0$ is larger for such semi-occlusion exercises that include a double source of vibration, i.e. water resistance exercises and lip or tongue trills, compared to the source exercises – e.g. phonation into a straw in air or humming. The result may be explained by methodological inaccuracies, as F_1 was derived from LPC analysis, which is known to be problematic, especially in the case of semi-occlusions like closed vowels, nasals, fricatives, etc. [29].

The experimental results for the male subject showed that during the water resistance exercise the oral pressure oscillated in synchrony with the water bubbling, and the vertical position of the larynx changed accordingly. The vocal fold vibration was also affected, as could be deduced from the EGG signal showing variation of the relative contact time of the vocal folds. These results are in line with other experimental studies, e.g. [17-19, 30]. Recently, the effect of water resistance exercising on vocal fold vibration has been confirmed by ultra-high-speed filming [31].

4.2 Comparison of the theoretical results with the experimental results

The first acoustic resonance frequency $F_1 = 200$ Hz computed for the resonance tube with the distal end in air (see Table 2) agrees very well with the first formant frequency 190 Hz found experimentally for the male VT (see Table 3) as well as with $F_1 = 190$ Hz found for the female VT in the earlier study by the authors [16]. Similarly, the computed bandwidth 19.2 Hz for the formant F_2 (see Table 1) is also in good agreement with the formant bandwidth 16 Hz obtained in the previous measurements [16].

The computed frequency F_m , which corresponds to the mechanical resonance, decreased from the assumed value $F_m = 66$ Hz for the VT without any tube [13] down to $F_m \cong 21$ -23 Hz for the VT with the resonance tube, and decreased further down with the distal end of the tube in water to $F_m \cong 8$ Hz, and to $F_m \cong 9$ -10 Hz for the Lax Vox tube (see Tables 1 and 2). These values are close to the bubbling frequency $F_b \cong 11$ -11.5 Hz found experimentally (see Table 3). It is also possible to hypothesize that during a complicated bubbling process, the mechanical resonance frequency F_m jumps between two values, which theoretically correspond to the phonation through the tubes into air ($F_m \cong 21$ -23 Hz) and into water ($F_m \cong 8$ -10 Hz) (see Tables 1 and 2). These jumps can reflect the changes of the radiation impedance Z_{RAD} at the distal end of the tube in air and in water, i.e. the changes of the boundary condition (4) during the creation of a new air bubble in water and just after the bubble separation from the tube orifice (see Fig. 6). Theoretically, in the cases studied, such frequency jumps of the mechanical resonance for the resonance tube would be between $F_m = 8$ Hz for water at the distal end of the tube, and $F_m = 23$ Hz for air at the distal end of the tube (see Table 2). This frequency interval covers the measured bubbling frequency $F_b = 11$ -11.5 Hz (see Table 3) as well as the interval of the bubbling frequencies $F_b = 11.2$ -20.5 Hz measured for 14 subjects phonating into a resonance tube with the distal end 2 cm and 10 cm in water (see [30]).

The first computed acoustic resonance frequency decreased from $F_1 \cong 200$ Hz for the tube end in air down to about $F_1 \cong 175$ Hz for the tube end in water (see Table 2), which agrees with the first formant frequency $F_1 \cong 179$ Hz found experimentally for the male VT (see Table 3). Similarly, the second acoustic formant frequency at about $F_2 \cong 330$ -340 Hz, obtained from the measurement of the male subject phonating into the tube with the distal end submerged in water (see Table 3), is in relatively good agreement with the computed second acoustic resonance frequency $F_2 = 368$ Hz (see Table 2).

The 3 dB frequency bandwidths $B_I \cong 135$ Hz and 117 Hz of the first acoustic resonance F_I measured from the spectra in Fig. 9 for 10 cm and 2 cm water depth, respectively, are higher than the bandwidth $B_I \cong 75$ Hz computed for the tube end in water (see Tables 1 and 3). Because the bandwidth $B_I \cong 138$ Hz measured for the tube end in air (see Tab. 3) is also considerably wider than the computed bandwidth $B_I \cong 70$ Hz (see Tab. 1), another source of damping from another yielding wall inside the human vocal tract should be taken into account in a next study, e.g. the effect of the cheeks.

5. Conclusions

The presented mathematical model of acoustic-structural interaction confirmed that the vibration of the laryngeal tissues during water resistance exercise can be substantially supported by a low frequency acoustic-structural (mechanical) resonance of the vocal tract, because it was shown that this resonance for phonation through the tube into water exists in the frequency range of bubbling. The tube immersion depths between 2 cm and 10 cm in water had a negligible effect on the peak-to-peak values of the oral pressure, the resonance frequencies of the coupled acoustic-structural system respecting the yielding walls in the vocal tract, or the bubbling frequency.

The intervals for the bubbling frequencies and the mechanical resonance frequencies overlap, so a strong vibration of the larynx (or only the vocal fold tissue) can be expected if both these frequencies merge. The coalescence of the bubbling frequency and the low acoustic-structural resonance frequency of the vocal tract could thus enhance the positive effects of the water therapy procedure, i.e. to intensify the massage-like effect that may potentially relax the muscles and improve liquid circulation in the tissue. The hypothesis of the enhancement of the bubbling effect by the yielding walls of the human vocal tract is also supported by the fact that the SPL of the oral pressure at the bubbling frequency is comparable with the SPL at the fundamental frequency.

On the other hand, the coalescence of the bubbling frequency and the low acoustic-structural resonance frequency of the vocal tract may result in unpleasantly intensive vibrations of the laryngeal tissues, which may even cause some vocal fold impairments. This is still an open question and a more detailed investigation is needed to establish safety recommendations for the use of water resistance voice therapy.

Acknowledgements

The study was supported by a grant from the Czech Science Foundation: No. 16-01246S “Computational and experimental modelling of self-induced vibrations of vocal folds and influence of their impairments on human voice”.

References

- [1] A.M. Laukkanen, About the so called "resonance tubes" used in Finnish voice training practice. An electroglottographic and acoustic investigation on the effects of this method on the voice quality of subjects with normal voice, *Scandinavian Journal of Logopedics and Phoniatrics* 17 (1992) 151-161.
- [2] I.R. Titze, E.M. Finnegan, A.M. Laukkanen, S. Jaiswal, Raising lung pressure and pitch in vocal warm-ups: The use of flow-resistance straws, *Journal of Singing* 58 (2002) 329-338.
- [3] S. Simberg, A. Laine, The resonance tube method in voice therapy: description and practical implementations, *Logopedics Phoniatrics Vocology* 32 (2007) 165-170.

- [4] I.R. Titze, B.H. Story, Acoustic interactions of the voice source with the lower vocal tract. *Journal of the Acoustical Society of America* 101 (1997) 2234-2243.
- [5] I.R. Titze, Voice training and therapy with a semi-occluded vocal tract: rationale and scientific underpinnings, *J Speech Lang Hear Res.* 49 (2006) 448-459.
- [6] I.R. Titze, A.M. Laukkanen, Can vocal economy in phonation be increased with an artificially lengthened vocal tract? A computer modeling study, *Logopedics Phoniatrics Vocology* 32(4) (2007) 147-156.
- [7] I.R. Titze, Acoustic interpretation of resonant voice. *Journal of Voice* 15 (2001) 519-528.
- [8] B.H. Story, A.M. Laukkanen, I.R. Titze, Acoustic impedance of an artificially lengthened and constricted vocal tract, *Journal of Voice*, 14, (2000) 455-469.
- [9] M.M. Sondhi, J. Schroeter, A hybrid time-frequency domain articulatory speech synthesizer, *IEEE Transactions on Acoustics, Speech and Signal Processing*, ASSP-35 (1987) 955-967.
- [10] M.M. Sondhi, Model for wave propagation in a lossy vocal tract, *Journal of the Acoustical Society of America* 55 (1974) 1070-1075.
- [11] O. Fujimura, J. Lindqvist, Sweep-Tone Measurements of Vocal-Tract Characteristics, *Journal of the Acoustical Society of America* 49 (1971) 541-558.
- [12] K. Ishizaka, J.C. French, J.L. Flanagan, Direct determination of vocal tract wall impedance, *IEEE Transactions on Acoustics, Speech and Signal Processing*, ASSP – 23 (1975) 370-373.
- [13] J. Liljencrants, *Speech Synthesis with a Reflection-Type Line Analog (PhD. dissertation)*, Stockholm (1985).
- [14] J.G. Švec, J. Horáček, F. Šram, J. Veselý, Resonance properties of the vocal folds: in vivo laryngoscopic investigation of the externally excited laryngeal vibrations, *Journal of the Acoustical Society of America* 108(4), (2000) 1397-1407.
- [15] V. Radolf, J. Horáček, A.M. Laukkanen, Comparison of computed and measured acoustic characteristics of an artificially lengthened vocal tract. In Manfredi, C. (ed.), *Models and Analysis of Vocal Emissions for Biomedical Applications – Proceedings, MAVEBA 2013*. Firenze: Firenze University, 2013, pp. 51-53. ISBN 978-88-6655-469-1.
- [16] V. Radolf, J. Horáček, P. Dlask, Z. Otčenášek, A. Geneid, A.M. Laukkanen, Measurement and mathematical simulation of acoustic characteristics of an artificially lengthened vocal tract, *Journal of Sound and Vibration* 366 (2016) 556-570.
- [17] L. Enflo, J. Sundberg, C. Rømedahl, A. McAllister, Effects on Vocal Fold Collision and Phonation Threshold Pressure of Resonance Tube Phonation With Tube End in Water, *Journal of Speech, Language, and Hearing Research* 56 (2013) 1530–1538.
- [18] S. Granqvist, S. Simberg, S. Hertegård, S. Holmqvist, H. Larsson, P.A. Lindestad, M. Södersten, B. Hammarberg, Resonance tube phonation in water: High-speed imaging electrographic and oral pressure observations of vocal fold vibrations – a pilot study, *Logopedics Phoniatrics Vocology*, Early Online: 1-9, (2014), DOI:10.3109/14015439.2014.913682.
- [19] G. Wistbacka, J. Sundberg, S. Simberg, Vertical laryngeal position and oral pressure variations during resonance tube phonation in water and in air. A pilot study, *Logopedics Phoniatrics Vocology* 41(3) (2015) 1-7.
- [20] H. Mori, H. Ohsawa, T.H. Tanaka, E. Taniwaki, G. Leisman, K. Nishijo, Effect of massage on blood flow and muscle fatigue following isometric lumbar exercise, *Medical Science Monitor* 10 (2004) CR173-178.
- [21] P. Weerapong, P.A. Hume, G.S. Kolt, The mechanisms of massage and effects on performance, muscle recovery and injury prevention, *Sports Medicine* 35 (2005) 235-256.
- [22] L. Davidson, E.H. Amick, JR., Formation of gas bubbles at horizontal orifices, *A.I.C.H.E. Journal* 2(3) (1956) 337-342.
- [23] V. Radolf, *Direct and Inverse Task in Acoustics of the Human Vocal Tract (PhD. thesis)*, Czech Technical University in Prague, 2010.
- [24] Z. Škvor, *Acoustics and Electro-Acoustics*, Academia, Praha, 2001.
- [25] T. Vampola, J. Horáček, J.G. Švec, FE modeling of human vocal tract acoustics. Part I: Production of Czech vowels, *Acta Acustica united with Acustica* 94 (2008) 433-447.

- [26] V. Radolf, J. Horáček, V. Bula, A.M. Laukkanen, Air-pressure characteristics and visualization of bubbling effect in water resistance therapy, in: V. Fuis (Ed.), *Engineering Mechanics 2014*. Brno University of Technology, 2014, pp. 528-531. ISBN 978-80-214-4871-1. ISSN 1805-8248.
- [27] M. Guzman, C. Castro, S. Madrid, C. Olavarria, M. Leiva, D. Muñoz, E. Jaramillo, A-M. Laukkanen, Air pressure and contact quotient measures during different semioccluded postures in subjects with different voice conditions, *Journal of Voice* in press, <http://dx.doi.org/10.1016/j.jvoice.2015.09.010>.
- [28] P. Amarante, G. Wood, P. Ratchliffe, R. Epstein, A. Pijper, J. Svec, Electroglossographic study of seven semi-occluded exercises: lax-vox, straw, lip-trill, tongue-trill, humming, hand-over-mouth, and tongue-trill combined with hand-over-mouth, *Journal of Voice* 28(5) (2014) 589-595.
- [29] R.E. Remez, K.R. Dubowski, M.L. Davids, E.F. Thomas, N.U. Paddu, Y.S. Grossman, M. Moskalenko, Estimating speech spectra for copy synthesis by linear prediction and by hand, *Journal of the Acoustical Society of America*, 130(4) (2011) 2173–2178.
- [30] J. Tyrmi, V. Radolf, J. Horáček, and A.M. Laukkanen, Resonance Tube or Lax Vox?, *Journal of Voice*, Vol. ■■, No. ■■, pp. ■■-■■, 0892-1997, <http://dx.doi.org/10.1016/j.jvoice.2016.10.024>.
- [31] M. Guzman, A.-M. Laukkanen, L. Traser, A. Geneid, B. Richter, D. Muñoz, M. Echternach, Effect of water resistance therapy on vocal fold vibration: A high speed registration study, *Logopedics Phoniatrics Vocology* in press. Published online: 02 Aug 2016, <http://dx.doi.org/10.1080/14015439.2016.1207097>.

Appendix

Procedure for determination of the formant frequencies

Acoustic analysis of the measured microphone signals during phonation was performed by using Matlab in several steps as follows.

1) Computation of the frequency spectra of the signal $y(t)$ for the length of several seconds using the fast Fourier transform (FFT) procedure and a Hanning window of length 1 s with an overlap of 75%:

$$Y_i(f) = FFT(hann\ y_i(t)). \quad (A1)$$

2) Calculation of the average spectrum from all spectra obtained in Step 1:

$$Y(f) = \frac{1}{N} \sum_{i=1}^N Y_i(f) \quad (A2)$$

3) Calculation of the mean value from the spectrum in $Y(f)$ in the frequency band $f \in \langle 0; F_0 \rangle$:

$$Y_{filt}(F_0/2) = mean(Y(f \in \langle 0; F_0 \rangle)) \quad (A3)$$

where F_0 is the fundamental phonation frequency.

4) Calculation of the average value of the spectrum $Y(f)$ in the frequency band $f \in \langle \Delta f, F_0 + \Delta f \rangle$:

$$Y_{filt}(F_0/2 + \Delta f) = mean(Y(f \in \langle \Delta f; F_0 + \Delta f \rangle)) \quad (A4)$$

where $\Delta f_s \leq \Delta f \leq F_0$ and Δf_s are the frequency steps in the spectra $Y_i(f)$ given by the length of the Hanning window used for the signal $y_i(t)$.

5) Calculation of the average value of the spectrum $Y(f)$ in the frequency band

$$f \in \langle 0 + 2\Delta f, F_0 + 2\Delta f \rangle:$$

$$Y_{filt}(F_0/2 + 2\Delta f) = mean(Y(f \in \langle 2\Delta f; F_0 + 2\Delta f \rangle)). \quad (A5)$$

6) Repeat the previous step up to the end of the considered frequency range.

By this procedure, the multiples of the fundamental frequency F_0 are suppressed in the resulting spectrum. The maxima of the function $Y_{filt}(f)$ are considered as formants, and the peaks in this spectrum determine the formant (resonance) frequencies.

The average FFT spectra in Fig. 9 were computed for $F_0 = 98$ Hz, with the frequency step of $\Delta f = 10$ Hz.